Scapular morphology variation affects reverse total shoulder arthroplasty biomechanics. A predictive simulation study using statistical and musculoskeletal shoulder models

Pavlos Silvestros, George S. Athwal, Joshua W. Giles

2024

Received: 13 April 2023 | Revised: 11 September 2023 | Accepted: 20 January 2024

DOI: 10.1002/jor.25801

Journal of Orthopaedic Research®

RESEARCH ARTICLE

Scapular morphology variation affects reverse total shoulder arthroplasty biomechanics. A predictive simulation study using statistical and musculoskeletal shoulder models

Pavlos Silvestros[1] | George S. Athwal[2] | Joshua W. Giles[1]

[1]Department of Mechanical Engineering, University of Victoria, Victoria, British Columbia, Canada

[2]Division of Shoulder and Elbow Surgery, Department of Orthopaedic Surgery, Roth/McFarlane Hand and Upper Limb Centre, London, Ontario, Canada

Correspondence

Joshua W. Giles, Department of Mechanical Engineering, University of Victoria, 3800 Finnerty Road, Victoria, BC, Canada.
Email: jwgiles@uvic.ca

Funding information

Micheal Smith Health Research British Columbia Scholar Award, Grant/Award Number: SCH-2021-1562; Institute of Musculoskeletal Health and Arthritis, Canadian Institutes of Health Research, Project Grant, Grant/Award Number: PJT-173505

Abstract

Reverse total shoulder arthroplasty (RTSA) accounts for over half of shoulder replacement surgeries. At present, the optimal position of RTSA components is unknown. Previous biomechanical studies have investigated the effect of construct placement to quantify mobility, stability and functionality postoperatively. While studies have provided valuable information on construct design and surgical placement, they have not systematically evaluated the importance of scapular morphology on biomechanical outcomes. The aim of this study was to assess the influence of scapular morphology variation on RTSA biomechanics using statistical models, musculoskeletal modeling and predictive simulation. The scapular geometry of a musculoskeletal model was altered across six modes of variation at four levels (±1 and ±3 SD) from a clinically derived statistical shape model. For each model, a standardized virtual surgery was performed to place RTSA components in the same relative position on each model then implemented in 50 predictive simulations of upward and lateral reaching tasks. Results showed morphology affected functional changes in the deltoid moment arms and recruitment for the two tasks. Variation of the anatomy that reduced the efficiency of the deltoids showed increased levels of muscle force production, joint load magnitude and shear. These findings suggest that scapular morphology plays an important role in postoperative biomechanical function of the shoulder with an implanted RTSA. Furthermore a "one-size-fits-all" approach for construct surgical placement may lead to suboptimal patient outcomes across a clinical population. Patient glenoid as well as scapular anatomy may need to be carefully considered when planning RTSA to optimize postoperative success.

KEYWORDS

musculoskeletal model, predictive simulations, reverse total shoulder arthroplasty, virtual surgery and statistical shape model

1 | INTRODUCTION

Currently, reverse total shoulder arthroplasty (RTSA) accounts for the majority of all shoulder replacement surgeries between 2015 and 2022 in the United States of America (52%),[1] and for 58% in the United Kingdom[2] and over 80% in Australia[3] for the year of 2021. Indications for RTSA include cuff tear arthropathy, glenohumeral osteoarthritis, massive rotator cuff tears and revision arthroplasty[2] which highlights the versatility of this surgical procedure. The popularity and versatility of this arthroplasty is largely due to the purported biomechanical advantages RTSA provides to patients postoperatively. These include a medialised joint center of rotation and improved deltoid efficiency as primary shoulder movers by increasing their effective moment arms and resting length as well as increased joint pre-compression improving joint stability over a large range of motion.[4] The benefits and versatility of RTSA have driven the development of many construct designs and surgical techniques to best address the pathologic population[2,5]; however, this presents surgeons with the challenge of selecting the implant design and placement on the glenoid (e.g., correcting inclination, version or level of lateralization of the glenosphere) to suit the patient's individual pathologic anatomy and desired functionality postoperatively.

Experimental and computational studies have evaluated the effects of the RTSA design parameters and component placements on biomechanical outcome variables.[6–10] Anatomic variation between patients is also an important factor that influences surgical planning and related outcomes but to date it has not been thoroughly addressed in the literature. Factors such as a patient's natural morphological variation of the scapula and pathomechanical adaptation of the glenoid fossa result in different relative positions of the glenohumeral joint from the acromion, scapula spine and coracoid. These anatomic factors in-turn affect the biomechanical characteristics of the native and postoperative joint (e.g., moment arms, muscle lengths, joint position, version and inclination). The altered biomechanics in turn contribute to postoperative function and construct loading,[6] thus contributing a major role to the success of the surgery. Although some studies have investigated patient cohorts to sample the population and estimate the biomechanical outcomes,[11] no studies have systematically investigated the effects of variations in specific morphological characteristics on outcome biomechanics. Thus, the relationships between scapular morphology and RTSA biomechanics remain unknown.

Musculoskeletal (MSK) modeling and predictive simulation software, such as OpenSim[12,13] and OpenSim Moco,[14] are powerful tools that can evaluate the causal relationships between changes to the musculoskeletal system (e.g., surgery) and its resulting function (e.g., motion and neuromuscular recruitment strategies) to achieve specific tasks. Such simulations do not require prior experimental kinematic or neural (e.g., electromyography) data to drive the model to produce motion; instead, they estimate the model's required neural commands to achieve a defined task given certain physiological and biomechanical objective functions and constraints. This property of predictive simulations guarantees that the generated kinematics are achievable by the model of the altered system by respecting the musculoskeletal system dynamics and task constraints as well as allowing for variation that may occur from surgical musculoskeletal alteration. A previous study has used this type of method to investigate the effect of shoulder capsuloraphy stiffness.[15]

Statistical shape models (SSMs) are a computational anatomy method that can efficiently describe variation in geometric datasets such as a clinical population's bony anatomy.[16] Previous studies have identified associations between scapular morphology and shoulder joint pathologies, such as critical shoulder angle and rotator cuff tears,[17,18] and others speculate that the large variance seen in acromion morphologies could be a main contributor in the development of shoulder pathology[11] that is regularly treated with RTSA.[2] This combined with the increasing use of SSMs in MSK modeling studies to better understand the function of the lower limb[19–21] illustrates that an SSM can be a powerful tool to systematically vary the geometry of musculoskeletal models to approximate population variance in scapular morphologies of interest, which can then be used in theoretical simulations.

Therefore, the first scientific aim of our study was to systematically evaluate the effect of scapular morphology variation on postoperative RTSA biomechanics when controlling for implant configuration by using constant implant parameters and constant relative surgical construct placement. Second, the technological goal was to develop a computational framework that can be used to predict the effect of patient morphology and construct placement on resulting biomechanics postoperatively using SSMs, musculoskeletal models, and predictive simulations. It was hypothesized that morphological changes would affect joint loading, muscle moment arms and muscle coordination during functional motions after RTSA.

2 | METHODS

The methodological process of this computational study was separated into four phases (Figure 1): (A) systematically generating scapular geometries from an SSM, (B) positioning implant constructs in a reference configuration through a virtual RTSA surgery, (C) redefining musculoskeletal model parameters based on the virtual surgery and (D) implementing the MSK models in predictive simulations to achieve tasks replicating activities of daily living (ADLs).

2.1 | Scapular geometry generation

A previously developed SSM,[22] optimized for scapular characteristics and developed through nonrigid registration processes, was used to generate sets of scapular morphologies based on a sample of 39 CT scans of patients undergoing RTSA. Twenty-five scapular morphologies were generated by independently varying each of six modes of variation of the SSM through four levels (±1 and ±3 SD) plus one morphology with weights of zero for all modes to yield the population average. Modes were chosen from the overall SSM that

most significantly varied the morphology of the glenoid fossa, acromion process, scapular spine and coracoid process (Table 1 and Figure 2) as these were believed to most strongly affect glenohumeral biomechanics. The nominal modes presented here as Modes 1–6 were the SSM's principal components (PC) ranked 2, 4, 5, 6, 7 and 9 (Table 1). The mode of variation affecting size (PC 1) was held constant at the mean value and the mode affecting glenoid erosion was held constant such that negligible erosion was present.

The varied morphologies were exported as stereolithography (STL) files that were registered to the baseline OpenSim model's[23] scapular geometry (discussed in Section 2.3: Musculoskeletal modeling) to obtain the relative orientation of the scapula on the thorax. Registering the generated geometries was completed in Python (version 3.10.5) using the VTK toolbox (version 9.2.2) through a six-point anatomic landmark rigid registration followed by an iterative closest point registration.

A set of vertices were manually indexed on the population average geometry that corresponded to the scapular muscle attachment sites with guidance from the baseline OpenSim model geometry and muscle atlases. Two additional sets of vertices were indexed on the glenoid rim and the supraspinatus fossa. The three sets of indexed vertices were used in the next step to identify

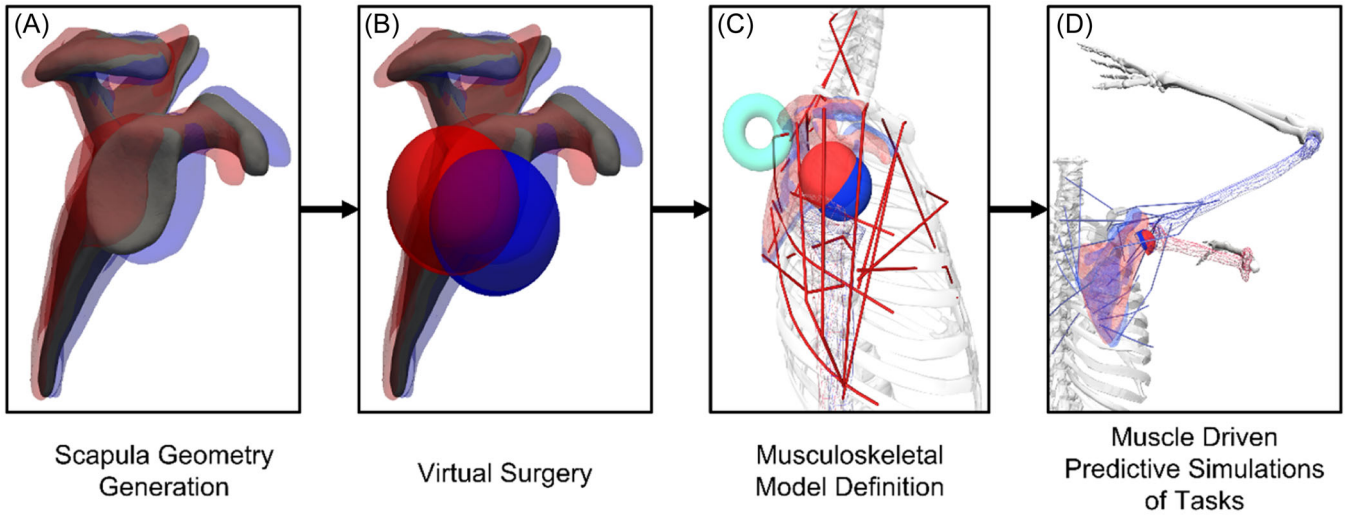

FIGURE 1 Schematic of the research methods from scapula geometry generation through to predictive simulation of ADL tasks. (A) 3D scapula geometry generation with SSM and mode of variation perturbation (gray: average; red: −3 SD; blue: +3 SD. (B) Virtual surgery computationally positioning parametric approximation of RTSA components based on orthopaedic surgeon guidelines performed for each geometry. (C) Definition of the musculoskeletal model for each perturbed scapular geometry, muscle attachment and joint locations (the additional torus wrapping surface for the lower trapezius is also visible). (D) Each model implemented in predictive simulations of two activities of daily living. For additional visualization of scapula morphology variation see Appendix (Figures S10–S15). ADL, activities of daily living; RTSA, reverse total shoulder arthroplasty; SSM, statistical shape model.

TABLE 1 Description of modes of scapula morphological variation.

Mode of variation	Primary morphological change (correlation[a])	Secondary morphological change (correlation[a])	Principal component rank[a]
Mode 1	Lateral acromion to glenoid center distance (0.62)	Coracoid tip to glenoid center distance (0.48)	2nd
Mode 2	Superior anterior acromion to glenoid center distance (0.66)	Posterior inferior acromion to glenoid center distance (0.64)	4th
Mode 3	Glenoid-acromion angle (0.87)	Glenoid-acromion-coracoid angle (−0.83)	5th
Mode 4	Coracoid tip to glenoid center distance (−0.53)	Lateral acromion to glenoid center distance (−0.43)	6th
Mode 5	Version angle (0.78)	Critical shoulder angle (−0.42)	7th
Mode 6	Acromial tilt angle (0.80)	Critical shoulder angle (0.61)	9th

Note: The anatomical changes are interpreted as the SD increases (−3 to +3 SD) red to blue.

[a]Rank and correlation related to the principal components identified in the SSM by Sharif-Ahmadian et al. (2023).[22]

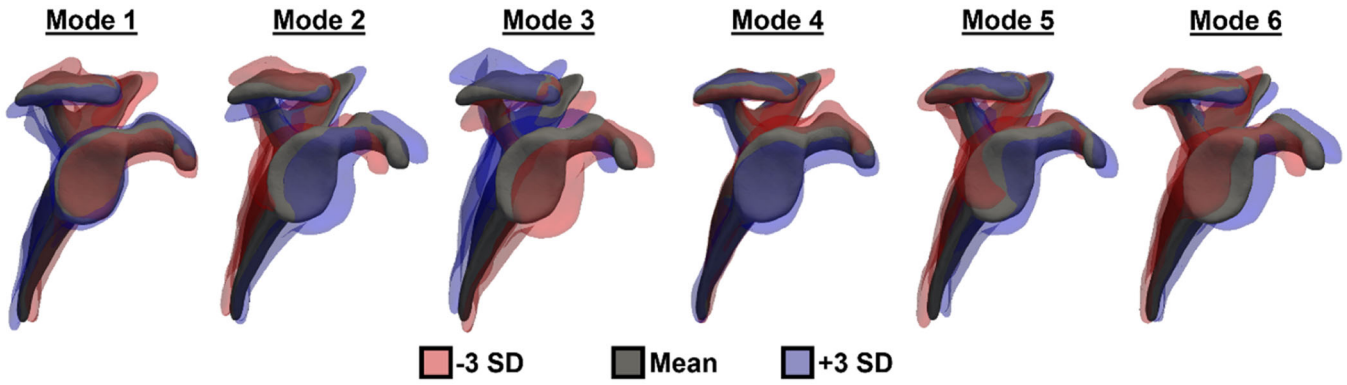

FIGURE 2 Visual representation of the six modes of variation used with ±3 SD instances of each. Constrained at the acromioclavicular joint. For additional visualization of scapula morphology variation see Appendix (Figures S10–S15).

biomechanical and geometrical parameters by utilizing the SSM's corresponding vertex indexing property across the generated geometries. This property ensures that each individual vertex is in the same relative geometrical location in each geometry instance across all possible variations allowing for automatic identification across all 25 geometries.

2.2 | Virtual surgery

A parametric computational method in Matlab 2022a (The Mathworks Inc.) and OpenSim 4.3 was developed for identifying scapular geometric properties, selecting and positioning RTSA implant components, defining a postoperative glenohumeral joint and creating a new musculoskeletal model.

Each geometry instance that corresponded to a varied scapular morphology analyzed in the previous phase was imported into Matlab as was the baseline humerus geometry from the OpenSim 4.3 model.[23] For each scapula STL a plane of best fit was calculated from all the 3D points of the geometry to define the scapula plane.[24] Similarly, the saved set of glenoid rim vertices identifying the 3D points of the glenoid rim were used to define the glenoid plane. Finally, the indexed vertices of the supraspinatus fossa were used to define a transverse scapular axis vector.

A glenoid reference system was defined with its origin at the barycenter of the glenoid rim vertices. The glenoid plane's normal vector was defined as the Z-axis directed laterally from the glenoid barycenter. A vector parallel to the intersection of the glenoid and scapular planes was defined as the Y-axis directed superiorly from the glenoid barycenter. The X-axis was defined as the Y- and Z-axis cross product. This axis definition followed the OpenSim model convention (X: anterior/posterior; Y: superior/inferior and Z: medial/lateral). The glenoid reference system was used to handle the positioning of the RTSA glenospheres.

To alter the joint anatomy to represent a reverse shoulder the size, positioning and orientation of the parametric hemisphere geometries, replicating the articulating surface of a standard (non-eccentric) glenosphere component of an RTSA implant, was chosen for all simulations following expert orthopaedic surgeon guidelines (GSA) as described in the following. The average height and width of the generated glenoids were measured and a 39 mm diameter glenoid hemisphere was chosen for all simulations. Superior glenoid inclination (10.8° ± 2.8°), calculated as the angle between glenoid Z-axis and transverse scapular vector projected on the Y-Z glenoid plane, was corrected through inferiorly rotating the glenosphere by the respective angle (Figure 3). Posterior glenoid version (17.1° ± 3.3°), calculated as the angle between the glenoid Z-axis and the transverse scapular vector projected on the X-Z glenoid plane, was not corrected. For each simulation the glenosphere was positioned to achieve a 7 mm inferior overhang and 2 mm lateralization from the inferior most point of the glenoid rim to the medial plane of the glenosphere as specified by expert surgical guidance (GSA).[25]

Across all models the humeral component remained the same. A parametric cup geometry was defined with the same radius to the glenosphere following RTSA designs with a humeral head cut plane of 135°.

The translational and angular offsets calculated in the previously described process for both the glenosphere and humeral cup components were used in the OpenSim API to define MSK models based on the virtual surgery for each of the 25 variations. The placement of the RTSA construct on the average geometry used in the MSK model can be seen in right of Figure 3.

2.3 | Musculoskeletal modeling

The baseline musculoskeletal model used for the study was the Wu shoulder model.[23] The seven segment MSK model maintained the inertial properties as in Wu et al.[23] It was assumed that the acromioclavicular joint location would remain constant across all varied scapulae. Therefore, all scapulae were connected to the baseline model at that joint completing the kinematic chain. The rotator cuff muscles were removed to simulate a complete cuff tear as this is a common primary diagnosis for RTSA procedures (18.1% in United States[1]; 51.2% in United Kingdom[2];

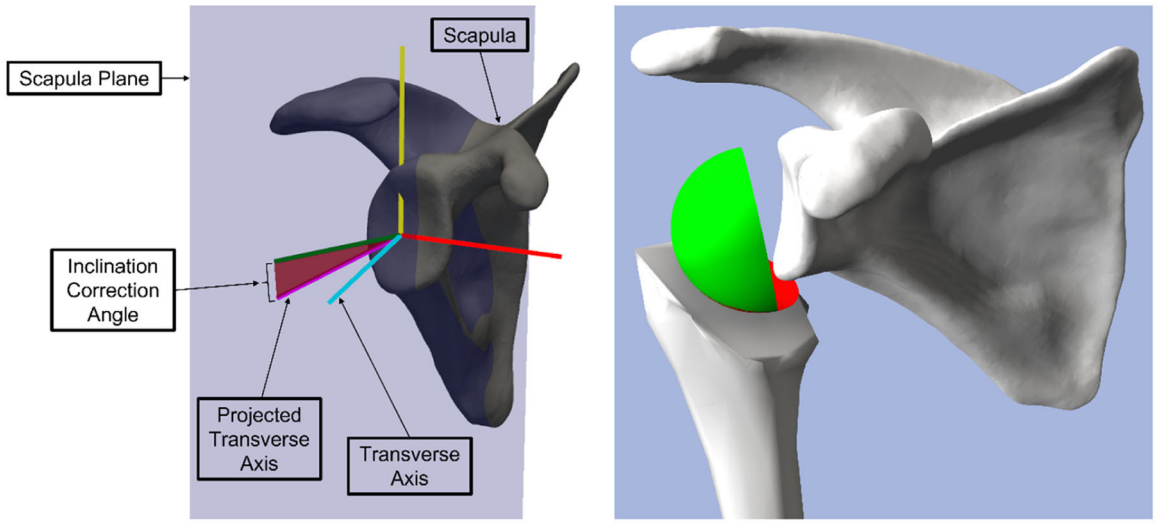

FIGURE 3 The mean scapula from the SSM[22] with the glenoid reference system used to handle the position and orientation of the glenosphere (left) and the resulting RTSA construct placements following the virtual surgery (right). Left: The glenoid reference system used to handle the position and orientation of the glenosphere is presented as the orthogonal system as X (red)—anterior/posterior, Y (yellow)—superior/inferior, Z (green)—medial/lateral. The defined scapula plane (blue) was used to orientate the glenoid Y-axis. The transverse axis of the scapula (cyan), calculated from the direction of the supraspinatus fossa, was projected on the glenoid YZ plane (magenta vector). The angle between the projected transverse axis and the glenoid Z-axis was defined as the inclination correction angle (rotation about the glenoid X-axis) by which the glenosphere was orientated. Right: The final placement of parametric surfaces of the RTSA glenosphere (green) and humeral cup (red) is presented on the musculoskeletal model's body segments of the scapula and humerus. RTSA, reverse total shoulder arthroplasty; SSM, statistical shape model.

36.3% in Australia[3]) resulting in a total of 22 musculotendon units (MTUs) that actuated the scapulothoracic and glenohumeral joints. The 3D location of scapular muscle attachment sites were redefined for each varied scapular morphology using the indexed vertices. This ensured that for each model the MTUs attachment sites were in the same relative position across the varied morphologies.[26]

Paths for four MTUs were altered to obtain stable and representative results. First, a torus was included for the lower trapezius muscle (TRAP4). Second, as RTSA significantly alters the moment arms of the deltoid muscles the muscle paths in the baseline MSK model were altered using via points to better reflect data from simulated post-RTSA surgery[26] (Appendix). The positions of the optimized via points were calculated only on the MSK model with the average scapular morphology and registered to the scapula's reference system for all other models to maintain the via points in the same relative location. All MTUs were then defined as DeGrooteFregly muscle models[27] to allow for the predictive simulations that followed. Elbow and wrist joints were driven by ideal torque actuators, with the torso locked with respect the ground.

2.4 | Predictive simulations of ADLs

Each MSK model defined with the varied scapular morphology was used in a predictive simulation procedure of two ADLs using OpenSim Moco.[14] OpenSim Moco allows for predictive muscle driven simulations by estimating the required muscle activation signals (i.e., control signals) to achieve a defined task by solving an optimal control problem using direct collocation methods.

The two ADL tasks chosen were unloaded forward reach and lateral reach. For the model to achieve these tasks computationally, an objective function was developed and passed to the optimizer. The objective function required the optimizer to: (a) minimize simulation time bounded between 0.75 and 2.5 s as observed in similar tasks from Bergman et al.,[28] (b) minimize effort (average sum of controls squared) and (c) to minimize the 3D end-point spatial error between markers defined on the model's end effector (i.e., hand segment) and target markers defined in 3D space. The target markers were projected laterally and anteriorly from the resting shoulder joint position at a distance of twice the length of the model's forearm for the lateral and forward reaching tasks, respectively, similarly to Fox et al.[15] All simulations started with the arm resting in the neutral position by the side of the torso and ended at rest at the target position. Ranges of shoulder joint motion collected experimentally[29] were used to adjust the RTSA MSK model's capabilities and to bound its shoulder coordinate values during simulations. A total of 50 (25 models × 2 tasks) predictive simulations converged to an optimal solution (dynamic constraint error less than 10^{-3}) each with an average simulation time of 3.5 h on a 12th Generation Intel i9 CPU.

2.5 | Biomechanical outcome variables

Post-RTSA muscle kinematics, joint kinematics and dynamics were calculated through OpenSim 4.3 analysis modules from the predicted simulations along with muscle moment arms, force and activations. Additionally, a joint loading ratio[6] was calculated (Equation 1).

$$FR = \frac{\sqrt{F_C^2}}{\sqrt{F_{AP}^2 + F_{SI}^2}}, \quad (1)$$

where F_C is compression, F_{AP} is anterior/posterior shear, and F_{SI} is superior/inferior shear.

3 | RESULTS

For each of the two simulated tasks (25 simulations each) the predicted kinematics of the converged simulations of the RTSA shoulder followed similar trajectory paths respecting the kinematic bounds defined in the optimization problem (Figure 4). For the upward and lateral reaching tasks shoulder elevation and shoulder rotation kinematics showed the least variation across all conditions.

Modes of morphologic variation dictated functional changes in anterior, middle and posterior deltoid muscle moment arms across the tasks (Figures 5–8, left columns). Throughout upward reaching (Figures 5 and 6, left columns), shoulder elevation moment arms increased with higher levels (i.e., from −3 to +3 SD) of Modes 2, 3, and 6 for the anterior deltoid and Modes 1, 3, and 6 for the middle deltoid. Elevation plane moment arms increased in Modes 3, 4, and 5 for the anterior deltoid (agonistically >0 mm) and Modes 1, 2, and 6 for the middle deltoid (antagonistically <0 mm). For lateral reaching (Figures 7 and 8, left columns), shoulder elevation moment arms increased in Modes 1, 2, 3, and 6 and Modes 3 and 6 for the middle and posterior deltoid respectively. The moment arm of the posterior deltoid transitioned into an adductor (antagonistically <0 mm) in the early stages of the movement in +3 and −3 SD for Modes 4 and 5, respectively. Elevation plane moment arms increased in Modes 1, 2, and 6 for both middle and posterior deltoids.

Muscle activation (Figures 5–8, center columns) dictated force generation (Figures 5–8, right columns) for each respective task's prime movers as they followed similar patterns. An inverse pattern of muscle force generation and moment arm change within modes of variation could be seen in Modes 1, 2, and 3 for the anterior deltoid during upward reaching. Similarly, during lateral reaching in Modes 2, 4, and 6 for the middle deltoid.

Resultant joint reaction forces showed more observable differences in Modes 3, 4, and 6 for upward reaching (Figure 9) and Modes 1, 2, 3, and 6 for lateral reaching (Figure 10). The joint loading ratio indicated that increased levels of Modes 4, 5, and 6 reduced relative shear loading whereas Modes 1, 2, and 3 increased relative shear (FR → 0) during upward and lateral reaching.

4 | DISCUSSION

This predictive simulation study evaluated the effect of scapular morphology variation on postoperative RTSA kinematics, joint function and loading. Variation in scapular morphology produced marked changes in the resulting biomechanics following the standardized RTSA placement for the two simulated tasks of ADLs, supporting our initial hypothesis. This overall finding is unsurprising, but this work is the first to systematically demonstrate this effect and indicates that the use of standardized implant placement may not produce equivalent functional outcomes across patients. The responses to the different modes of variation were dependent on

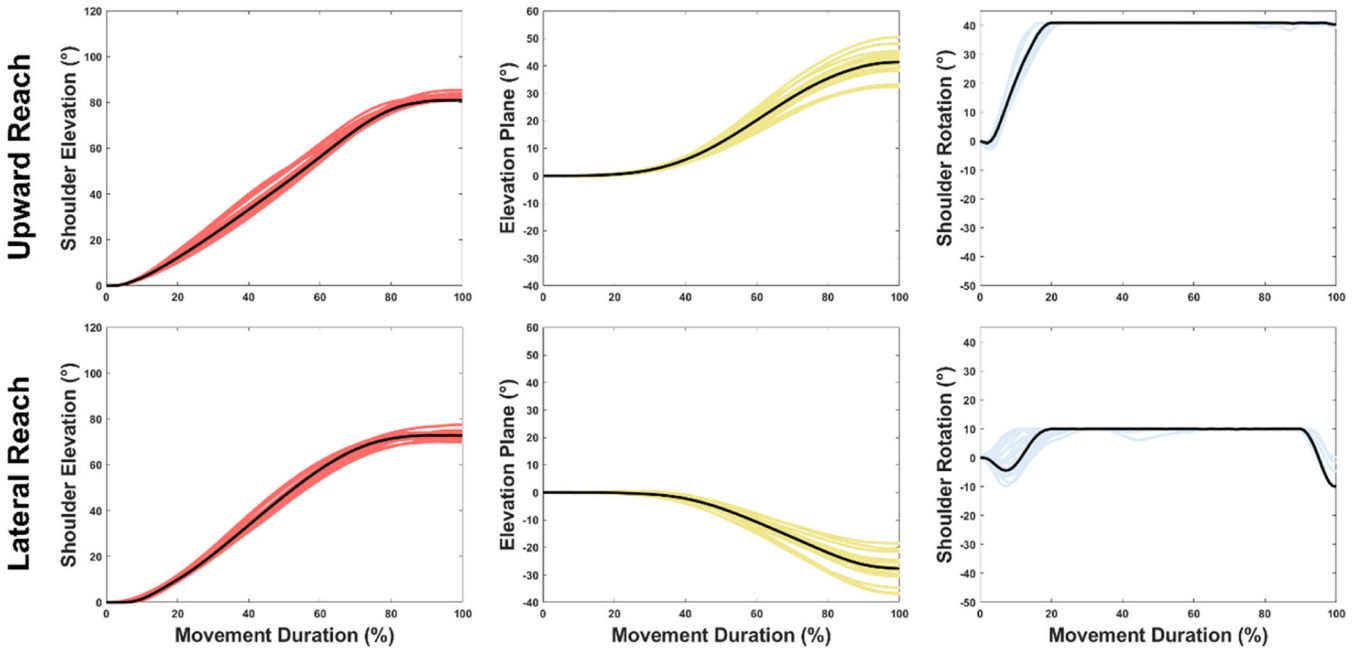

FIGURE 4 Shoulder joint kinematics across all tasks (rows) and joint coordinates (columns) for all 50 simulations normalized to task duration (0%–100%). Joint kinematics from the average morphology for each task displayed in black.

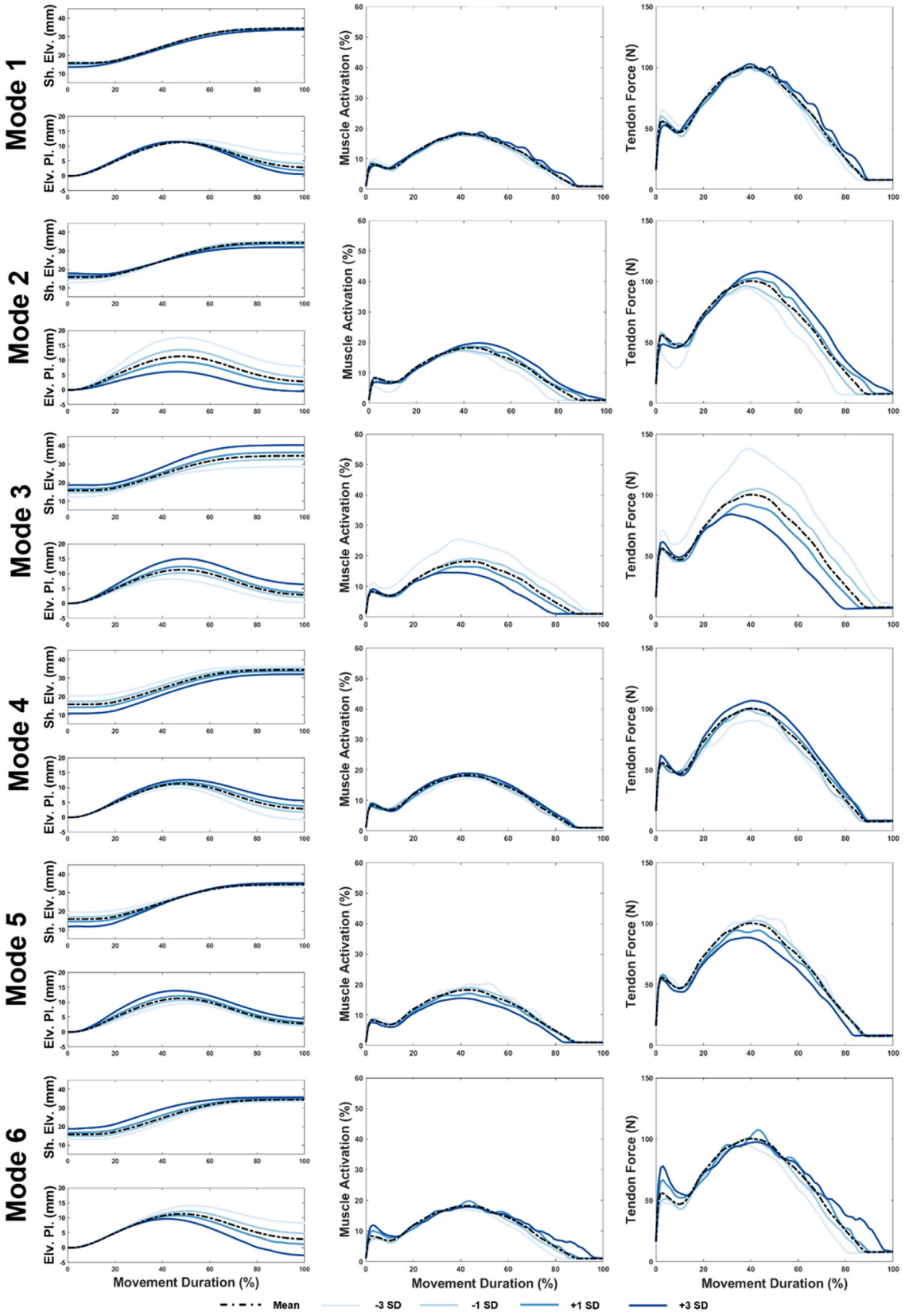

FIGURE 5 Muscle moment arms (left column) for shoulder elevation (top) and elevation plane (bottom; +ive/−ive = forward/backward flexion), muscle activations (center column) and total muscle force production (right column) normalized to % movement duration for each mode of variation (rows) and level of variation (light blue [−3 SD], dark blue [+3 SD] and black [average morphology]) for the anterior deltoid during the upward reaching task.

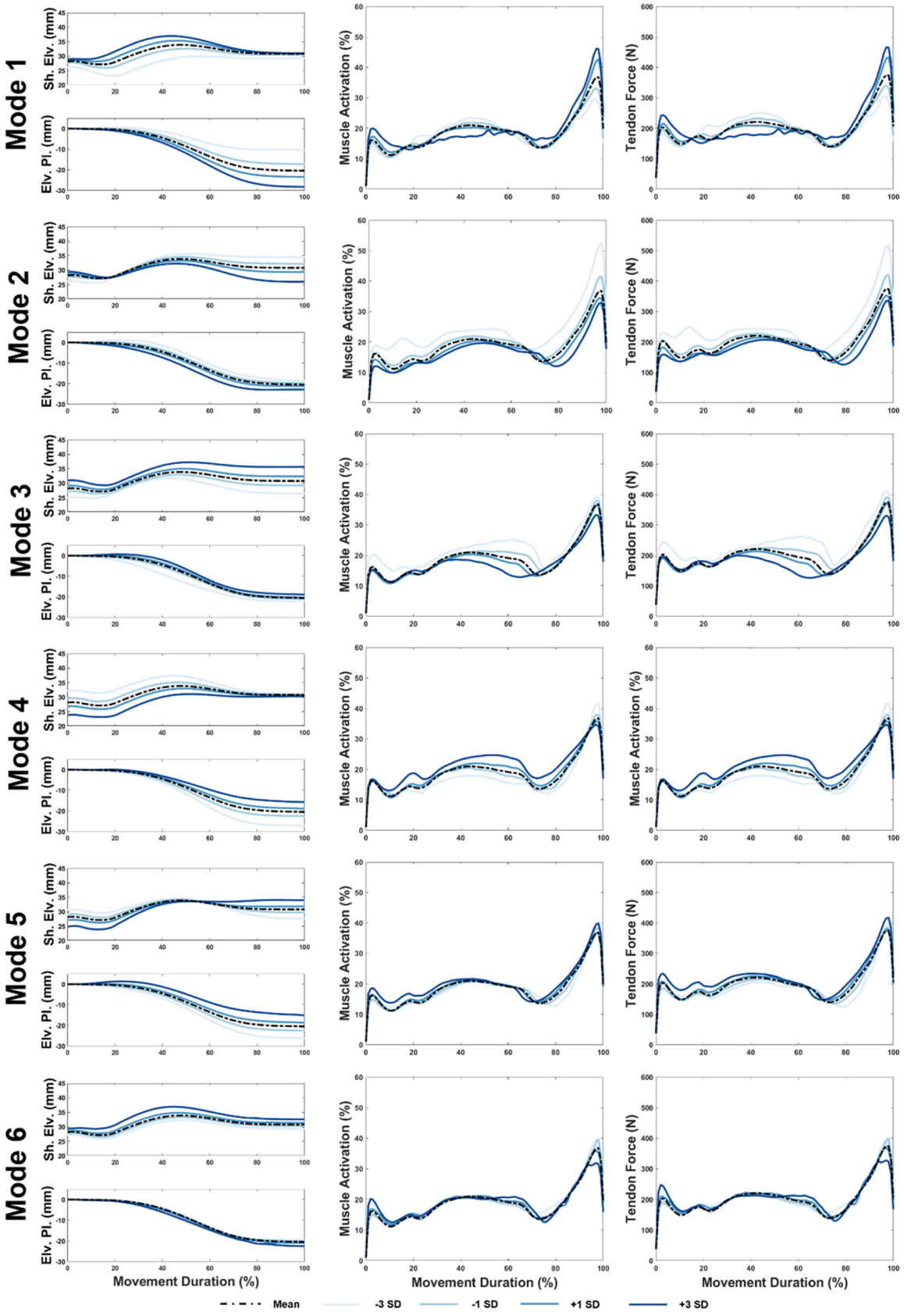

FIGURE 6 Muscle moment arms (left column) for shoulder elevation (top) and elevation plane (bottom; +ive/−ive = forward/backward flexion), muscle activations (center column) and total muscle force production (right column) normalized to % movement duration for each mode of variation (rows) and level of variation (light blue [−3 SD], dark blue [+3 SD] and black [average morphology]) for the middle deltoid during the upward reaching task.

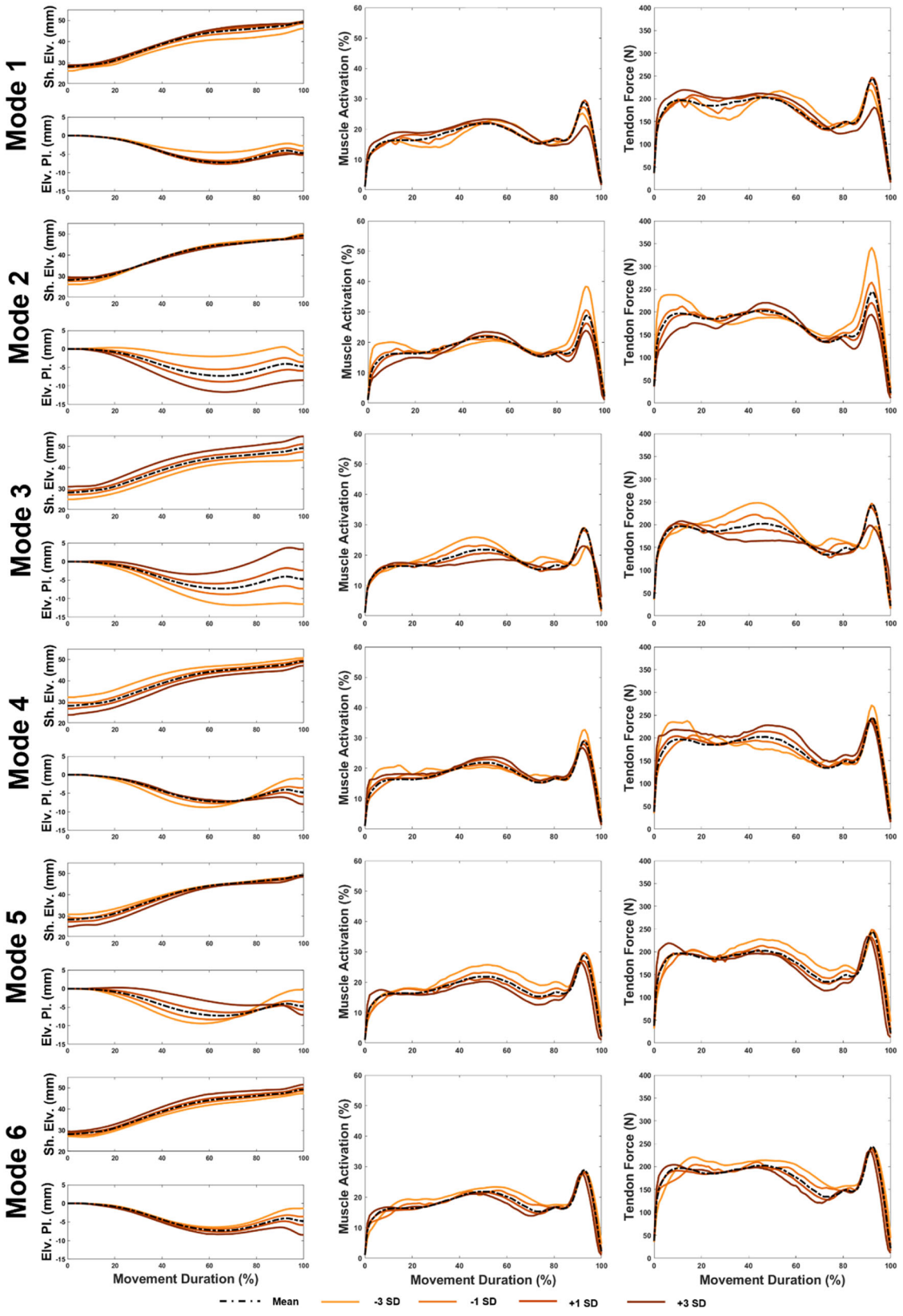

FIGURE 7 Muscle moment arms (left column) for shoulder elevation (top) and elevation plane (bottom; +ive/−ive = forward/backward flexion), muscle activations (center column) and total muscle force production (right column) normalized to % movement duration for each mode of variation (rows) and level of variation (light red [−3 SD], dark red [+3 SD] and black [average morphology]) for the middle deltoid during the lateral reaching task.

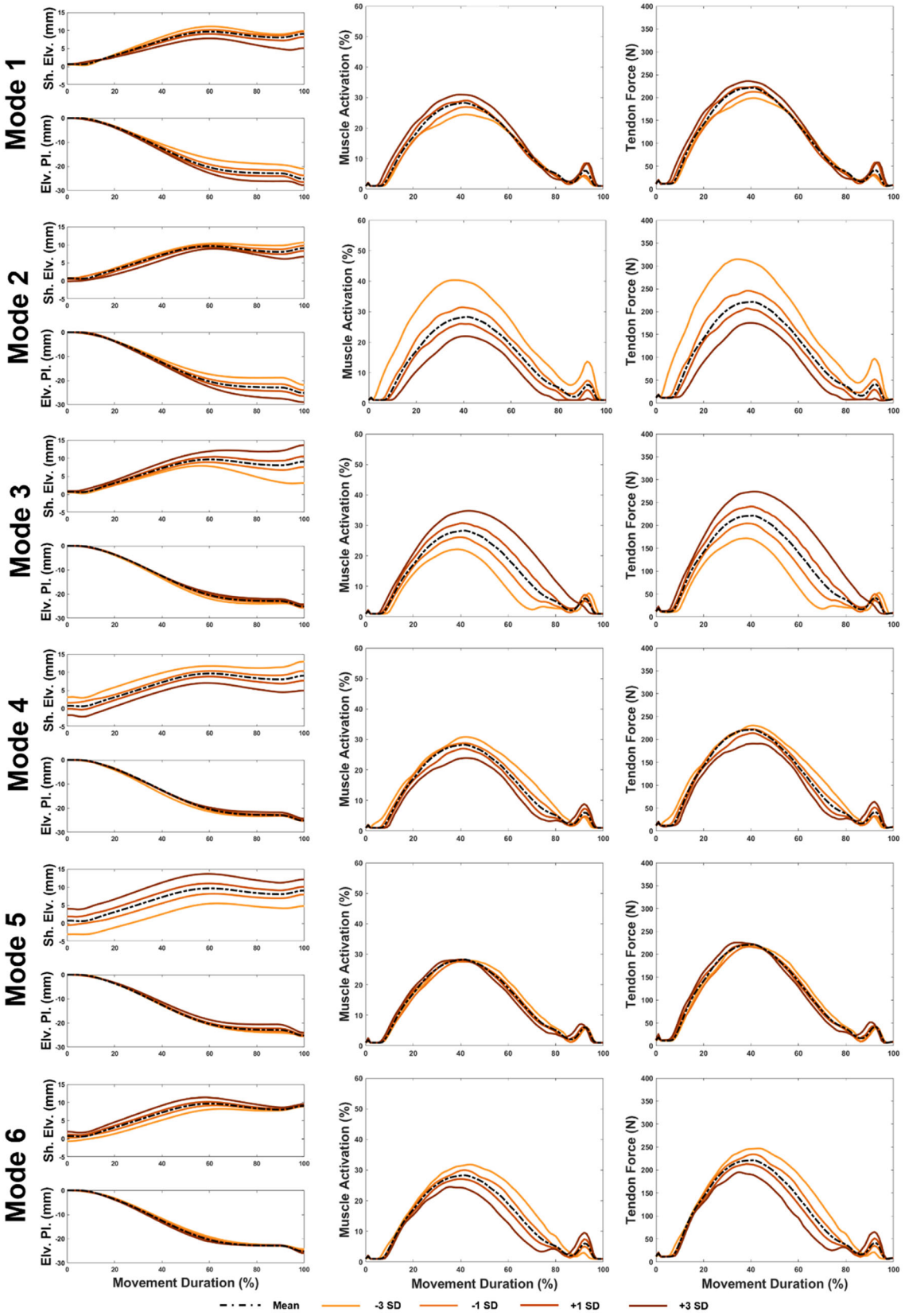

FIGURE 8 Muscle moment arms (left column) for shoulder elevation (top) and elevation plane (bottom; +ive/−ive = forward/backward flexion), muscle activations (center column) and total muscle force production (right column) normalized to % movement duration for each mode of variation (rows) and level of variation (light red [−3 SD], dark red [+3 SD] and black [average morphology]) for the posterior deltoid during the lateral reaching task.

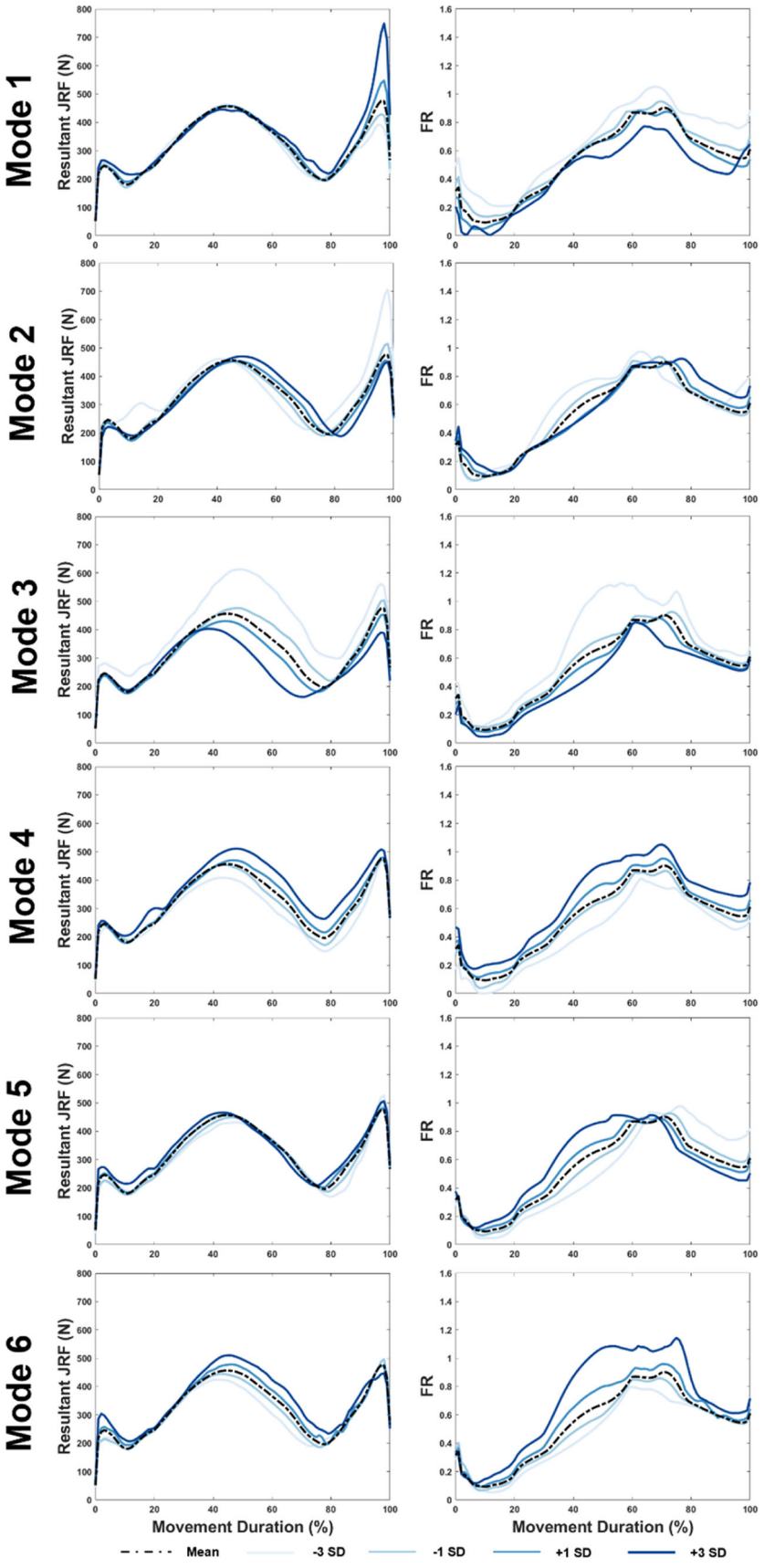

FIGURE 9 Resultant joint loads (left column) and force ratio (right column) for each mode of variation and level of variation (light blue [−3 SD], dark blue [+3 SD] and black [average morphology]) normalized to % movement duration in the upward reaching task.

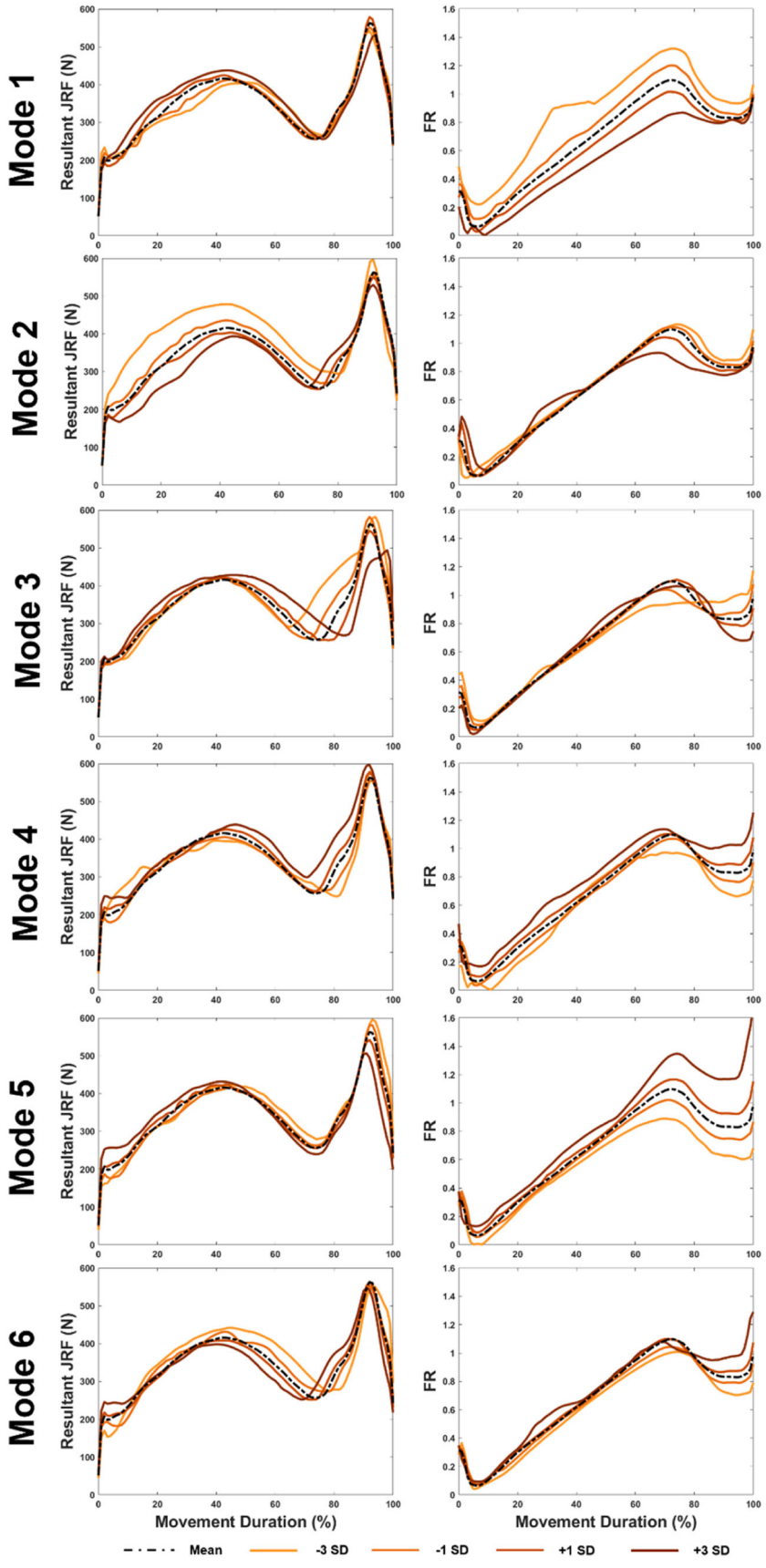

FIGURE 10 Resultant joint loads (left column) and force ratio (right column) for each mode of variation and level of variation (light blue [−3 SD], dark blue [+3 SD] and black [average morphology) normalized to % movement duration in the lateral reaching task.

specific morphological changes and the biomechanical requirements for each task. Interestingly, modes of morphological variation that changed the position of the glenoid and its relative distance from the acromion had larger effects on resulting biomechanics.

Scapular morphology changes had a small effect on the kinematic patterns and time of completions for each task. While joint kinematics and time did vary within each simulated task, the deviations were reflective of postoperative experimental kinematic[29] and temporal[28] variability for patients that underwent shoulder surgery. Additionally, maximal loading during simulated upward and lateral reaching were comparable to peak in vivo joint loads measured in total shoulder replacement patients during pure shoulder elevation (545.0 ± 150.2 N) and abduction (607.6 ± 146.6 N) tasks.[28] Our study simulated the effect of morphological variation on resulting biomechanics following a standardized virtual RTSA surgery. Although the joint kinematics did not vary significantly, the resulting joint loads displayed larger effects for specific morphological changes in the scapula. As a result, considering the functional biomechanical effect of scapular morphology should be an important factor in surgical decision making because standardized implant positioning that aims to place the constructs in the same relative manner across a patient population (a "one-size-fits-all" approach so to speak) does not lead to the same biomechanical results. It is important to note, that surgeons do currently consider scapular morphology during preoperative planning, but primarily to optimize implant fixation not to customize patient postoperative function as shown in this study.

Previous studies have correlated the relative shape variation of the acromion and glenoid to the risk of developing degenerative rotator cuff tear arthropathy,[17,18] however, the effect of these changes postoperatively have not been fully understood. The six scapular morphology modes varied in our study had various effects across tasks on the resultant glenohumeral joint loads. Morphologically, the modes were chosen as they displayed the largest changes to the periarticular anatomy of the scapula (e.g., glenoid position relative to the acromion). The effect of such morphological changes on postoperative joint loads in addition to previous findings identifying high contribution of similar modes in nonpathologic scapulae variation[11] highlight the clinical significance of periarticular anatomy to pre- as well as post-operative biomechanics of the glenohumeral joint. Combining scapular geometries from a clinical SSM into the MSK models provides a more physiologically plausible representation of a clinical populations' morphology that underwent RTSA compared to using geometries derived from a healthy population.

Functionally, the variation in these periarticular modes resulted in larger changes to the shoulder elevation and elevation plane moment arms of the shoulder's prime movers (*m. deltoids)* that in turn alters their mechanical efficiency to actuate the glenohumeral joint to achieve specific tasks. An intuitive example can be seen in upward reaching, where the prime movers are the anterior and middle deltoids; an inverse relationship between muscle moment arms and force generation is clearly observed for Mode 3. Specifically, as the relative position of the glenoid with respect to the acromion is lateralised (+3 to −3 SD) the anterior and middle deltoid moment arms for shoulder elevation and the elevation plane are decreased resulting in increased muscle recruitment (Figures 5 and 6) to achieve the same task. This pattern was also clear during lateral reaching in Mode 6 for the middle and posterior deltoids (Figures 7 and 8). However, the multiplanar nature of the deltoids, especially when lacking the rotator cuff and following RTSA, complicates this inverse relationship as was seen in other modes of variation. Furthermore, other more complicated ADL tasks that involve shoulder rotation about multiple axes and loading conditions (e.g., velocity, end effector weight etc.) may introduce complex nonlinear relationships between morphology and resulting biomechanics, that are less intuitive for clinicians to predict when conducting surgical planning. Thus, the influence of scapular morphology has the potential to have significant clinical relevance to RTSA planning and patient outcome measures as standardized surgical placement of RTSA constructs may not benefit all patients to the same level.

The resulting biomechanical differences identified by the musculoskeletal model can be associated with potential adverse postoperative clinical outcomes. Acromion and scapular spine stress fractures are still a concern for patients following RTSA.[30,31] Over tensioning of the deltoid active soft tissues surgically by placing constructs more inferiorly on the glenoid may predispose certain patients to such stress fractures if the resulting biomechanics are not considered. For Modes 3 and 4, muscle force increased with the relative acromion-glenoid distance. Repetitive loading of the acromion, especially in patients with poor bone quality, could result in accumulation of micro-damage and potential stress fracture. More work needs to be focused on matching clinical populations' muscle properties (e.g., strength, optimal fiber length and passive properties) to morphological changes to better explore the influence of muscle force generating properties on such results. Another informative outcome of the study is the directionality of the resulting joint load vector. As can be seen in the change of the Force Ratio (Figures 9 and 10) specific morphological changes increase the relative shear compared to compressive joint loading during ADLs. Such information can be used to identify high risk morphologies that would be susceptible to construct loosening or dislocation, and thus could inform future finite element analyzes and surgical planning tools.

Our study maintained a common relative configuration of the RTSA construct on the glenoid as scapular morphology was varied systematically across the 25 geometries from the SSM. This was done to remove the confounding factor of varying RTSA construct configuration and placement. This is the first study to our knowledge to systematically investigate the effect of scapula morphology on post-RTSA biomechanics. Previous studies have studied the impact of construct placement alterations with respect to a reference configuration without controlling for morphological effects[6,9,10,32] providing important information on the possible outcome of surgical decision and component design parameters. Glenday et al.[6] developed a musculoskeletal modeling framework that identified inferior glenosphere translation had the most beneficial biomechanical effects when considering deltoid length, moment arms, impingement free range of motion and joint stability. However, the scapular

morphologies used were a cross sectional sample of a healthy population that may not represent a clinical RTSA population. Furthermore, dynamic motions of ADL were not simulated as in the presented study. By generating the scapular morphologies used in our study's MSK model from a validated SSM[22] we were able to attribute specific geometrical changes in the MSK model (e.g., moment arms) and the resulting biomechanics during simulated activities of daily tasks to specific morphological changes of the scapula. The use of clinical SSMs is an important advancement in predictive surgery workflows as computational studies can strategically and systematically sample from a clinical population to identify morphologies that could be high risk to complications postoperatively.

By combining computational anatomy, musculoskeletal modeling and predictive simulations our study has demonstrated that computational biomechanical frameworks can systematically assess the effect of changes to the musculoskeletal system, such as in orthopaedic surgery, on resulting biomechanics during functional tasks of the upper limb. This supports previous studies that utilized forward driven predictive simulations[15] to evaluate the possible result of surgical decision factors on postoperative biomechanical function. Utilizing predictive musculoskeletal simulations in these frameworks has the benefit of assessing the musculoskeletal system's resulting dynamics that are not constrained to follow existing data which do not match the system under investigation, for example kinematics from healthy participant or previous clinical datasets of specific movements. This can be thought of as how individual systems can adapt their strategies to achieve the same final goal. The results presented in this study and the methodology utilized can be advanced in the future by including the RTSA component positioning modulation presented by Glenday et al.[6] In a following study, we aim to do so to investigate the interaction of clinically relevant scapular morphology variations with construct positioning and orientation to identify the optimal placement of RTSA constructs with respect to functional biomechanical outcomes. This may lead the way to advancing preoperative planning technologies—that currently provide only geometric guidance to surgeons (e.g., sizing, position and inclination/version of construct)—to include information of possible postoperative biomechanical function based on construct placement decisions and patient morphology.

5 | LIMITATIONS

As with any computational study a number of considerations must be taken into account. First, although the scapular morphologies and related muscle attachments were varied, whilst maintaining the overall size constant, the rest of the musculoskeletal models' geometry and muscle parameters were not varied. This was chosen to better relate morphological changes of the scapula to biomechanical results by reducing the amount of covariate parameters. Future studies would improve this by also modulating clavicle and humeral morphology and muscle attachment sites as well as shoulder girdle muscle parameters such as optimal muscle fiber lengths and maximal force generating capacity based on clinical populations. Second, the choice of terms in the cost function focused on task achievement and did not account for factors that may relate to pain, such as joint or muscle loading, that might be relevant to recovered RTSA patients. Thirdly, in line with previous shoulder modeling studies such as Glenday et al.[6], where RTSA was studied, and Fox et al.,[15] where capsuloraphy was studied, the scapulothoracic kinematics were not altered in the models' kinematic constraints which may not represent what happens with RTSA patients postoperatively as they can adopt movement adaptations to compensate for loss of function. As such this is another area for future work in the field as there is little consensus in the literature allowing for generalizable kinematic constraints to be used in such models. Finally, in our analysis we only looked at biomechanical functional outcome measures. Other factors such as impingement free range of motion are important metrics for surgical outcome performance as has been eloquently shown in the recent study by Glenday et al.[6]; however, this was outside the scope of this study.

6 | CONCLUSION

In summary, our study developed a predictive biomechanical framework to systematically investigate the effect of scapular morphology variations on biomechanical outcomes after RTSA surgery. In agreement with previous studies highlighting the importance of periarticular anatomy on the development of arthropathy, modes of variation that changed the relative positioning of the glenoid and acromion had the largest and most consistent effects. Importantly, we showed that a "one-size-fits-all" approach that does not personalize the placement of RTSA constructs by taking into account periarticular morphology variations is unlikely to yield optimal biomechanical outcomes across patients. Future studies should build on these results to see the combined effect of morphology, construct design, placement and muscle function on postoperative biomechanical results.

AUTHOR CONTRIBUTIONS

Conceptualization: Pavlos Silvestros, George S. Athwal, and Joshua W. Giles. *Methodology*: Pavlos Silvestros, George S. Athwal, and Joshua W. Giles. *Software*: Pavlos Silvestros. *Formal analysis*: Pavlos Silvestros. *Investigation*: Pavlos Silvestros, and Joshua W. Giles. *Resources*: Pavlos Silvestros, and Joshua W. Giles. *Data curation*: Pavlos Silvestros. *Writing—original draft preparation*: Pavlos Silvestros. *Writing – review and editing*. Pavlos Silvestros, George S. Athwal, and Joshua W. Giles. *Visualization*: Pavlos Silvestros. *Supervision*: Joshua W. Giles. *Funding acquisition*: Joshua W. Giles and George S. Athwal. All authors have read and approved the submitted manuscript.

ACKNOWLEDGMENTS

This study was funded by the Canadian Institutes of Health Research and through the Michael Smith Health Research British Columbia Scholar Award.

CONFLICT OF INTEREST STATEMENT

The authors declare no conflicts of interest.

ORCID

Pavlos Silvestros http://orcid.org/0000-0002-6588-7250
Joshua W. Giles http://orcid.org/0000-0001-6997-8873

REFERENCES

1. American Academy of Orthopaedic Surgeons (AAOS). 2022. Shoulder and Elbow Registry (SER): 2022 Annual Report. Rosemont, IL. [cited 2023 Mar 30] Available from: https://www.aaos.org/registries/publications/ser-annual-report/
2. National Joint Registry. 2022. 19th Annual Report. Hemel Hempstead, Hertfordshire [cited 2023 Mar 30] Available from: https://reports.njrcentre.org.uk/
3. Australian Orthopaedic Association National Joint Replacement Registry. 2022. Hip, knee & shoulder arthroplasty 2022 annual report. Adelaide, SA. [cited 2023 Mar 30] Available from: https://aoanjrr.sahmri.com/annual-reports-2022
4. Boileau P, Watkinson DJ, Hatzidakis AM, Balg F. Grammont reverse prosthesis: design, rationale, and biomechanics. *J Shoulder Elbow Surg*. 2005;14(1, suppl ment):S147-S161. Available from: https://www.sciencedirect.com/science/article/pii/S1058274604002903
5. Roche CP. Reverse shoulder arthroplasty biomechanics. *J Funct Morphol Kinesiol*. 2022;7(1):13. Available from: https://www.mdpi.com/2411-5142/7/1/13
6. Glenday J, Sivarasu S, Roche S, Kontaxis A. Development of a framework to assess the biomechanical impact of reverse shoulder arthroplasty placement modifications. *J Orthop Res*. 2022;40(9):2156-2168. Available from: doi:10.1002/jor.25238
7. Ackland DC, Patel M, Knox D. Prosthesis design and placement in reverse total shoulder arthroplasty. *J Orthop Surg*. 2015;10(1):101. Available from. doi:10.1186/s13018-015-0244-2
8. Ackland DC, Wu W, Thomas R, et al. Muscle and joint function after anatomic and reverse total shoulder arthroplasty using a modular shoulder prosthesis. *J Orthop Res*. 2019;37(9):1988-2003. Available from: doi:10.1002/jor.24335
9. Huish EG, Athwal GS, Neyton L, Walch G. Adjusting implant size and position can improve internal rotation after reverse total shoulder arthroplasty in a three-dimensional computational model. *Clin Orthop Relat Res*. 2021;479(1):198-204. Available from: https://journals.lww.com/clinorthop/Fulltext/2021/01000/Adjusting_Implant_Size_and_Position_Can_Improve.34.aspx
10. Giles JW, Langohr DGG, Johnson JA, Athwal GS. Implant design variations in reverse total shoulder arthroplasty influence the required deltoid force and resultant joint load. *Clin Orthop Relat Res*. 2015;473(11):3615-3626. Available from: https://journals.lww.com/clinorthop/Fulltext/2015/11000/Implant_Design_Variations_in_Reverse_Total.46.aspx
11. Jacxsens M, Elhabian SY, Brady SE, et al. Thinking outside the glenohumeral box: hierarchical shape variation of the periarticular anatomy of the scapula using statistical shape modeling. *J Orthop Res*. 2020;38(10):2272-2279. Available from: doi:10.1002/jor.24589
12. Delp SL, Anderson FC, Arnold AS, et al. OpenSim: open-source software to create and analyze dynamic simulations of movement. *IEEE Trans Biomed Eng*. 2007;54(11):1940-1950. Available from: https://www.ncbi.nlm.nih.gov/pubmed/18018689
13. Seth A, Hicks JL, Uchida TK, et al. OpenSim: simulating musculoskeletal dynamics and neuromuscular control to study human and animal movement. *PLoS Comput Biol*. 2018;14(7):e1006223. Available from: doi:10.1371/journal.pcbi.1006223
14. Dembia CL, Bianco NA, Falisse A, Hicks JL, Delp SL. OpenSim moco: musculoskeletal optimal control. *PLoS Comput Biol*. 2020;16(12):e1008493. Available from: doi:10.1371/journal.pcbi.1008493
15. Fox AS, Bonacci J, Gill SD, Page RS. Simulating the effect of glenohumeral capsulorrhaphy on kinematics and muscle function. *J Orthop Res*. 2021;39(4):880-890. Available from: doi:10.1002/jor.24908
16. Sarkalkan N, Weinans H, Zadpoor AA. Statistical shape and appearance models of bones. *Bone*. 2014;60:129-140 Available from. https://www.sciencedirect.com/science/article/pii/S8756328213004948
17. Spiegl UJ, Horan MP, Smith SW, Ho CP, Millett PJ. The critical shoulder angle is associated with rotator cuff tears and shoulder osteoarthritis and is better assessed with radiographs over MRI. *Knee Surg Sports Traumatol Arthrosc*. 2016;24(7):2244-2251 Available from. doi:10.1007/s00167-015-3587-7
18. Moor BK, Bouaicha S, Rothenfluh DA, Sukthankar A, Gerber C. Is there an association between the individual anatomy of the scapula and the development of rotator cuff tears or osteoarthritis of the glenohumeral joint? *Bone Joint J*. 2013;95-B(7):935-941. Available from: doi:10.1302/0301-620X.95B7.31028
19. Clouthier AL, Smith CR, Vignos MF, Thelen DG, Deluzio KJ, Rainbow MJ. The effect of articular geometry features identified using statistical shape modelling on knee biomechanics. *Med Eng Phys*. 2019;66:47-55. Available from: https://www.sciencedirect.com/science/article/pii/S1350453319300347
20. Van Rossom S, Wesseling M, Smith CR, et al. The influence of knee joint geometry and alignment on the tibiofemoral load distribution: a computational study. *Knee*. 2019;26(4):813-823. Available from: http://www.sciencedirect.com/science/article/pii/S0968016018305258
21. Bahl JS, Zhang J, Killen BA, et al. Statistical shape modelling versus linear scaling: effects on predictions of hip joint centre location and muscle moment arms in people with hip osteoarthritis. *J Biomech*. 2019;85:164-172. Available from: https://www.sciencedirect.com/science/article/pii/S0021929019300685
22. Sharif-Ahmadian A, Beagley A, Pearce C, Saliken D, Athwal GS, Giles JW. Statistical shape and bone property models of clinical populations as the foundation for biomechanical surgical planning: application to shoulder arthroplasty. *J Biomech Eng*. 2023;145(10):101004. Available from: doi:10.1115/1.4062709
23. Wu W, Lee PVS, Bryant AL, Galea M, Ackland DC. Subject-specific musculoskeletal modeling in the evaluation of shoulder muscle and joint function. *J Biomech*. 2016;49(15):3626-3634. Available from: https://www.sciencedirect.com/science/article/pii/S0021929016310107
24. Boileau P, Cheval D, Gauci M-O, Holzer N, Chaoui J, Walch G. Automated three-dimensional measurement of glenoid version and inclination in arthritic shoulders. *J Bone Jt Surg*. 2018;100(1):57-65. Available from: https://journals.lww.com/jbjsjournal/Fulltext/2018/01030/Automated_Three_Dimensional_Measurement_of_Glenoid.8.aspx
25. de Wilde LF, Poncet D, Middernacht B, Ekelund A. Prosthetic overhang is the most effective way to prevent scapular conflict in a reverse total shoulder prosthesis. *Acta Orthop*. 2010;81(6):719-726. Available from: doi:10.3109/17453674.2010.538354
26. Ackland DC, Roshan-Zamir S, Richardson M, Pandy MG. Moment arms of the shoulder musculature after reverse total shoulder arthroplasty. *J Bone Joint Surg Am*. 2010;92(5 Available from):1221-1230. https://journals.lww.com/jbjsjournal/Fulltext/2010/05000/Moment_Arms_of_the_Shoulder_Musculature_After.20.aspx
27. De Groote F, Kinney AL, Rao AV, Fregly BJ. Evaluation of direct collocation optimal control problem formulations for solving the muscle redundancy problem. *Ann Biomed Eng*. 2016;44(10):2922-2936 Available from. doi:10.1007/s10439-016-1591-9

28. Bergmann G, Graichen F, Bender A, et al. In vivo gleno-humeral joint loads during forward flexion and abduction. *J Biomech*. 2011;44(8):1543-1552. Available from: https://www.sciencedirect.com/science/article/pii/S002192901100265X
29. Vidt ME, Santago AC, Marsh AP, et al. The effects of a rotator cuff tear on activities of daily living in older adults: A kinematic analysis. *J Biomech*. 2016;49(4):611-617. Available from: https://www.sciencedirect.com/science/article/pii/S0021929016300513
30. Cho C-H, Jung J-W, Na S-S, Bae KC, Lee KJ, Kim DH. Is acromial fracture after reverse total shoulder arthroplasty a negligible complication? A systematic review. *Clin Orthop Surg*. 2019;11(4):427-435. Available from: doi:10.4055/cios.2019.11.4.427
31. Mahendraraj KA, Abboud J, Armstrong A, et al. Predictors of acromial and scapular stress fracture after reverse shoulder arthroplasty: a study by the ASES complications of RSA multicenter research group. *J Shoulder Elbow Surg*. 2021;30(10):2296-2305. Available from: https://www.sciencedirect.com/science/article/pii/S105827462100149X
32. Wong MT, Langohr GDG, Athwal GS, Johnson JA. Implant positioning in reverse shoulder arthroplasty has an impact on acromial stresses. *J Shoulder Elbow Surg*. 2016;25(11):1889-1895. Available from: https://www.sciencedirect.com/science/article/pii/S1058274616300660

SUPPORTING INFORMATION

Additional supporting information can be found online in the Supporting Information section at the end of this article.

How to cite this article: Silvestros P, Athwal GS, Giles JW. Scapular morphology variation affects reverse total shoulder arthroplasty biomechanics. A predictive simulation study using statistical and musculoskeletal shoulder models. *J Orthop Res*. 2024;1-16. doi:10.1002/jor.25801